Dynamic Mechanical Properties of Acrylic Rubber Blended with Phenolic Resin

Caiyun Wu, Chunyan Wei, Weihong Guo, Chifei Wu

Polymer Alloy Laboratory, School of Materials Science and Engineering, East China University of Science and Technology, 130 Meilong Rd., Shanghai 200237, People's Republic of China

ABSTRACT: The dynamic mechanical properties of blends of phenolic resin (PF) and acrylic rubber (ACM) were investigated. PF had good compatibility with ACM and played an important role in the damping of the ACM/PF blends. With the increase of PF content and molecular weight, the peak of loss factor (tan δ) of blends shifted to a higher temperature and became much wider, indicating the convenience to adjust the value of tan δ peak and the temperature range. Fourier Transform infrared spectroscopy detected that the intermolecular hydrogen bonding between the PF hydroxyl groups and the ACM carbonyl groups had made a great contribution to the improvement of damping. Compared with the organic small molecule used in our previous study, PF gifted the blends with equivalent damping performance and much better stability and a lower cost for the application of damping materials. © 2008 Wiley Periodicals, Inc. J Appl Polym Sci 109: 2065–2070, 2008

Key words: phenolic resin; acrylic rubber; dynamic mechanical analysis; damping

INTRODUCTION

Vibration often causes undesirable consequences,[1–3] such as unpleasant motions, noise, and dynamic stresses that lead to fatigue and failure of structures, decreased reliability and degraded performance. Polymers have been applied widely for achieving acoustic and vibration damping and isolation due to a unique combination of low modulus and inherent damping.[2,4–7] However, homopolymers usually exhibit efficient damping in a narrow temperature range of only 20–30°C around their glass transition temperatures (T_g), among which the polymers have pronounced dissipation of the mechanical energy as heat based on the onset of coordinated chain molecular motion.[8–10]

Traditional methods[2–13] of modification and broadening of the T_g involves use of copolymer, modified crosslinking agents, plasticizers and fillers, blending of various polymers, grafting and formation of interpenetrating polymer networks. Recently Chifei Wu[14–19] has found that organic hybrids, consisting of polar polymer, such as chlorinated polyethylene (CPE) or acrylic rubber (ACM), and functional organic small molecule substance such as 3,9-bis[1,1-dimethyl-2{β-(3-*tert*-butyl-4-hydroxy-5-methylphenyl) propionyloxy} ethyl]-2,4,8,10-tetraoxaspiro[5,5]-undane (AO-80), show novel energy dissipation peaks and high values of loss factor (tan δ) above T_g of matrix polymer, resulting from the formation of intermolecular hydrogen bonding. Great breakthrough has been made to provide a new concept of additive on damping performance.

Whereas these organic compounds with low molecular weights, some of which are very expensive, usually tend to be brittle and to transfer to the surface of the blends for a long-term. The high cost and instability of damping materials will lead to limited application. Phenolic resin (PF), just like AO-80 in chemical structure, contains a high density of hydroxyl groups that are able to interact with numerous other polymers through hydrogen bonding.[18–22] It is of great interest to take the place of those functional organic small molecules by PF as a kind of stable and economical additive on damping performance. In this study, the dynamic mechanical properties were investigated for a binary system consisting of ACM and PF, which was expected to be a good candidate for damping materials.

EXPERIMENTAL

Materials and sample preparation

ACM in this study was Nipol AR42W purchased from Nippon Zeon Corp. Details of PF with varying molecular weights (Asahi Organic Chemicals Industry Co.) are listed in Table I. AO-80, a kind of organic compound used as a contrast against PF, was a commercially available antioxidant (ADK STAB

Correspondence to: C. F. Wu (wucf@ecust.edu.cn).

TABLE I
Characteristics of PF Used

Code	Commercial name	$T_g{}^a$ (°C)	$M_n{}^b$	$M_w{}^b$	$M_w/M_n{}^b$	Softening point^c (°C)
PF (S)	CP506U	37.0	580	1780	3.06	95
PF (M)	SP1010	43.2	735	2870	3.90	104
PF (L)	SP1006	63.5	850	6000	7.05	120

^{a} Measured by DSC.
^{b} Measured by GPC.
^{c} ASTM E28-67.

AO-80, Asahi Denka Industries Co.). Chemical structures of PF and AO-80 are described as Figures 1 and 2, respectively.

After ACM was kneaded with a mixing roller for 5 min, powder of PF or AO-80 was added and the mixture was kneaded again at room temperature for 10 min to ensure homogeneity. The sheeted out stock was made molten for 3 min and then pressed at 130°C for 10 min under a pressure of 10 MPa. At the end of molding, the samples under compression were cooled to about 50°C by circulating water at ambient temperature through the platens to obtain samples 1.5 mm thick.

Differential scanning calorimetry

The T_g of materials was detected by a Netzch PC200 differential scanning calorimeter. Temperature was increased from room temperature to 100°C at a rate of 10°C/min. Samples were quenched and returned from −50 to 100°C at a rate of 10°C/min. Results of the second run were used for this study. The T_g is taken as the midpoint of the specific heat increment.

Dynamic mechanical analysis

The dynamic mechanical analysis was carried out on a UBM Dynamic Mechanical Analyzer Rheogel E-4000. Strips were cut in about 6 mm wide. All the measurements were performed from −40 to 100°C at a heating rate of 3°C/min under liquid nitrogen and at a fixed frequency of 11 Hz in tension mode.

Fourier transform infrared (FTIR) spectroscopy

Infrared spectra were obtained from an accumulation of 32 scans at a resolution of 1 cm^{-1} with a Nicolet Magna Model 550 infrared spectrometer. Attenuation reflection (ATR) mode was applied for the opaque specimens with a thickness of about 1.5 mm.

RESULTS AND DISCUSSION

The T_g is a very important factor associated with the onset of segmental mobility. The DSC responses of

the ACM and three kinds of PF are shown in Figure 3. All the materials are amorphous and give obvious single transitions. The T_g of ACM is -24.6°C, while PF exhibits T_g of 37.0, 43.2, and 63.5°C with the increase of softening point and molecular weight, respectively.

The temperature dependence of the loss factor (tan δ) for blends of ACM with PF(L) of different content is plotted in Figure 4. Table II presents detailed information related to tan δ peaks. Pure ACM has a high tan δ peak with a maximum approaching to 2.45. Its effective damping range with tan δ above 1.00 is relatively narrow from −17.8 to 5.8°C and is centered at −8.2°C, too low for general damping application.

In the hope of widening the effective damping temperature region and raising the temperature of tan δ peak, PF, with potentiality to form hydrogen bonding with carbonyl groups in the ACM, is introduced as additive. As shown in Figure 4, all the blends exhibit single tan δ peaks implying that ACM has good compatibility with PF(L) and no evident phase separation exists at these measurement conditions. With the addition of PF(L), the temperature of tan δ peak, usually taken as the T_g for damping materials, transfers from about −8°C to even 53°C. Moreover, the temperature range with tan δ above 1.00 grows much wider from 23 to 44°C, in despite of a more or less reduction of tan δ peak value. In
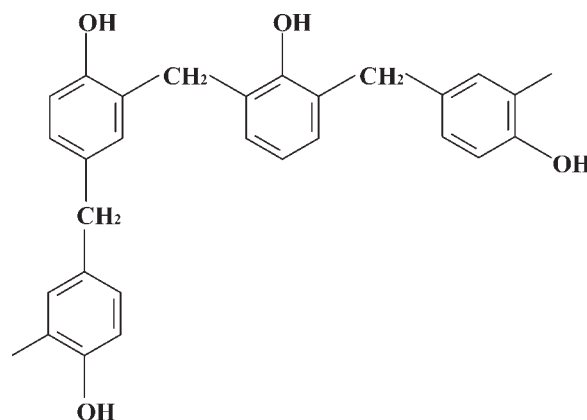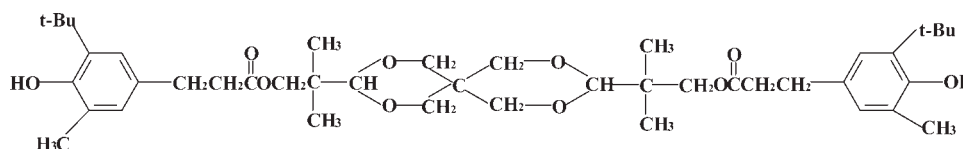

Figure 1   Chemical structure of PF.

Figure 2 Chemical structure of AO-80.

the case of ACM/PF(L)(50/50), it is remarkable that the tan δ peak is located at 53.5°C and the temperature range with tan δ above 1.00 is from 36.9 to 79.9°C. The improvement of damping performance of ACM caused by PF(L) is of great significance for further attempt to find out a new kind of additive on damping performance.

Figure 5 shows the temperature dependence of the storage modulus (E') for ACM and ACM/PF(L) blends. There is a notable drop in the storage modulus corresponding to the glass transition of the polymer systems. With the addition of PF(L), the modulus increases in the glassy region and performs in opposite way in the rubbery region. When the temperature is lower than a critical point, PF perhaps have the possibility to form a strong interaction of hydrogen bonding with ACM, besides just acting as reinforcing filler like carbon black or mica. As the temperature ascends, the intermolecular bonding is gradually destroyed and PF is contributed to diminishing ACM entanglements and a decreasing modulus.[20]

Dynamic mechanical properties of blends of ACM with PF(M) and PF(S) are explored as well, exhibiting the similar trends as that with PF(L) as a function of blend ratio, but difference exists among series of diversified PF. Effects of AO-80 on and tan δ of ACM has been reported in preliminary study.[1,14–19] With the addition of AO-80, the tan δ peak goes up significantly and moves to a higher temperature.
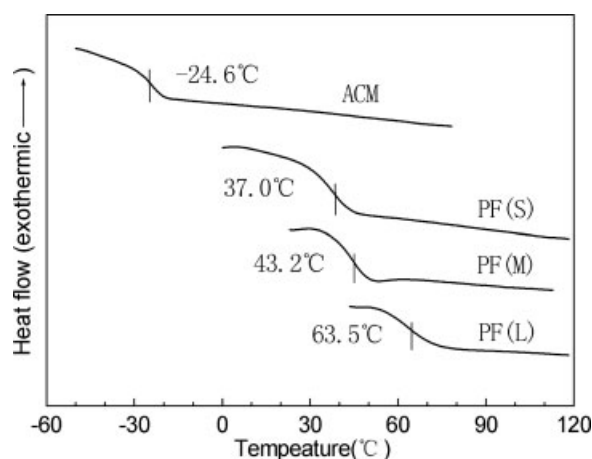
Samples of ACM/AO-80 are prepared here for a comparison with ACM/PF. Figures 6 and 7 give curves of the temperature dependence of tan δ and for ACM and binary blends of ACM containing 50 wt % AO-80 or different kinds of PF.

With the increase of molecular weight of PF, the broad tan δ peak shifts to a higher temperature and has a slight fall, while the modulus is close to each other, except for ACM/PF(S) with a relatively low one. The varying tan δ peak coincides with the increasing T_g of PF, and the modulus mainly depends on the molecular weight. Therefore, it is convenient to control the effective damping just by varying content and molecular weight of PF to meet practical demands.

Evident distinction is clarified between ACM/PF and ACM/AO-80. Table III lists the detailed information from Figure 6. ACM/AO-80 has a high top value of tan δ to 4.0 and a temperature range from 14.0 to 50°C with tan δ above 1.0. In the case of ACM/PF, the tan δ peak of ACM/PF is widened remarkably and located at a higher temperature with the maximum of tan δ around 2.00. Moreover, all the blends of ACM/PF get larger modulus and 20–30°C higher flowing temperatures, which are valuable parameters in the application. The improvement of effective temperature range of damping and flowing temperature of ACM/PF can be explained by the large molecular weight of PF, which also offers great
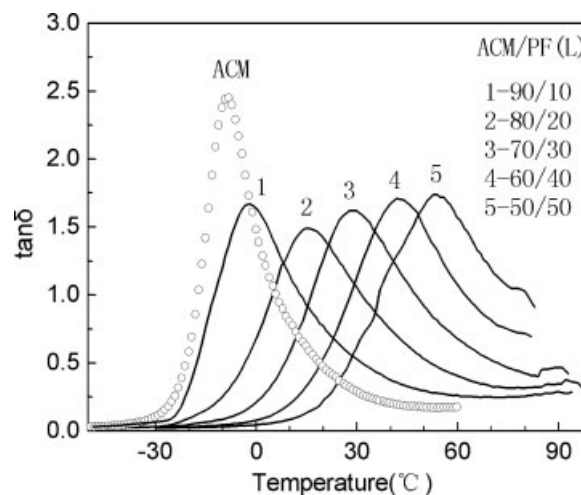

Figure 3 The DSC thermograms of ACM and various PF with different molecular weights.

Figure 4 Temperature dependence of loss factor (tan δ) at 11 Hz for ACM/PF(L).

TABLE II
Damping Performance for Blends of ACM With Different PF(L) Content

Wt. ratio ACM/PF(L)	tan δ peak value	tan δ peak temp. (°C)	Temp. range (°C) for tan δ > 1.00		
			T_1	T_2	ΔT
100/0	2.45	−8.2	−17.0	5.8	23
90/10	1.67	−2.1	−12.2	12.9	25
80/20	1.49	15.3	4.9	30.9	26
70/30	1.62	28.8	16.9	46.9	30
60/40	1.71	41.8	29.9	61.9	33
50/50	1.74	53.5	36.9	79.9	44

steric hindrance to reduce the height of tan δ peak as a result of great amounts of aromatic groups at the same time. Given a lower cost and more stability for a long-term, PF will be more attractive and competent than AO-80 in the application of damping materials.

Infrared spectroscopy has been proven as a powerful tool to investigate specific interaction between polymers and the mechanism of interpolymer miscibility through the formation of hydrogen bonding.[17–18,21–27] Figure 8 shows infrared spectra of carbonyl stretching measured at 25°C ranging from 1650 to 1800 cm^{-1} for pure ACM and various ACM/PF(L) blends.

The infrared carbonyl stretching for the pure ACM only gives a single band centered at 1734 cm^{-1}, corresponding to the free carbonyl groups. Another contribution at approximately 1690 cm^{-1} appeared as the presence of 10 wt % PF(L). Furthermore, the new band gets stronger and shifts to higher frequency with the increase of PF(L) content at 1700 cm^{-1}. Meanwhile, the intensity of the free carbonyl groups decreases gradually. The observation reveals the exact hydrogen bonding interaction between ACM

carbonyl and PF hydroxyl, which plays an important role to provide the excellent damping performance in a broad temperature range for the ACM/PF blends. Although difficult to calculate precisely, the fraction of hydrogen bonding mounts up obviously. The average strength of the intermolecular interaction[21] can be obtained by the extent of frequency difference (Δv) between the hydrogen bonded carbonyl absorption and free one. Figure 8 indicates that the average strength becomes weaker and goes saturated with the increasing PF content. It is resulted from enhanced effect of steric hindrance caused by more and more hydrogen bonding.[19,21] It could also explain the slight reduction of tan δ peak with increasing molecular weight of PF as shown in Figure 7. The larger the molecular weight of PF, the stronger influence of steric hindrance owing to aromatic groups among the polymer chains.

The hydroxyl-stretching region of the ACM/PF(L) blends is also examined. Figure 9 shows the infrared spectra in the 3000–4000 cm^{-1} corresponding to Figure 8. The pure ACM without hydroxyl has no response in the frequency range. A band centered at
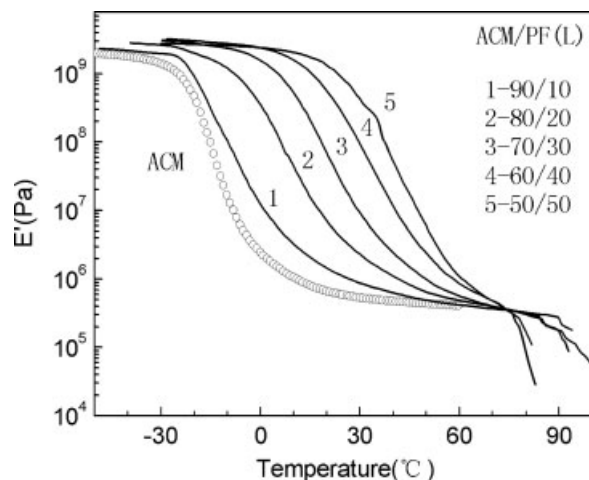

Figure 5 Temperature dependence of storage modulus (E') at 11 Hz for ACM/PF(L).
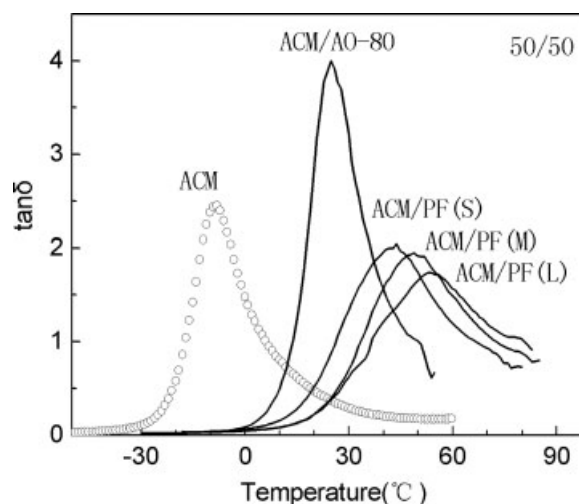

Figure 6 Temperature dependence of loss factor (tan δ) at 11 Hz for ACM and two binary systems of ACM/AO-80(50/50) and ACM/PF(50/50).
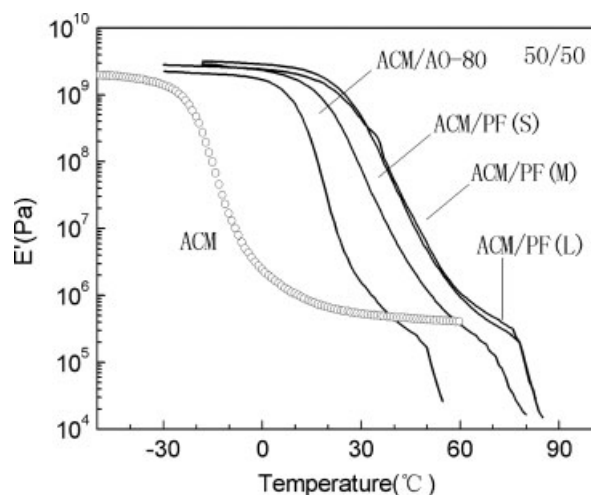
Figure 7 Temperature dependence of storage modulus (E') at 11 Hz for ACM and two binary systems of ACM/AO-80(50/50) and ACM/PF(50/50).
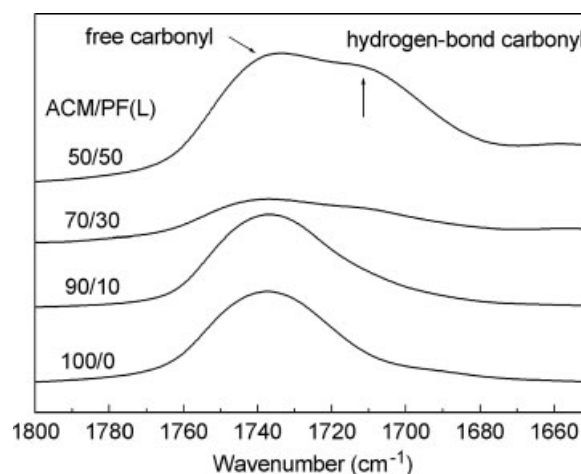

Figure 8 FTIR spectra recorded at 1800–1650 cm^{-1} region at 25°C for ACM/PF(L).

3400 cm^{-1} emerges as the addition of 10 wt % PF(L) in the blends. With the increase of PF(L) content, the band has the tendency to be split into two parts, shifting into higher and lower frequency, respectively. As is reported by Shiao Wei Kuo and Feng Chih Chang,[26,27] the PF is composed of two hydroxyl components, a very broad band centered at lower frequency attributed to the wide distribution of the hydrogen bonded hydroxyl group and a relatively narrow band at higher frequency caused by the free hydroxyl group. Additionally, the average strength of the hydrogen bonding between PF hydroxyl and polymer carbonyl is weaker than that of self-associated hydroxyl of PF and the former has a band located at higher frequency than the latter. It can be concluded that the intermolecular hydroxyl–carbonyl bond grows to intramolecular hydroxyl–hydroxyl bond with increasing PF(L) content, and more and more free hydroxyl group comes into being, indicating that there is hydrogen-bonding interaction between the ACM carbonyl group and the hydroxyl group of PF. These results are consistent with the dynamic mechanical properties discussed above.

CONCLUSIONS

The blends of ACM with PF were prepared to be a perfect kind of damping material with high-power and low-cost by simple process of mixing and molded compression. From the results of DMA, PF was compatible with ACM and acted as an excellent kind of additive on damping performance. The tan δ peak of the ACM/PF blends became much wider and shifted to a higher temperature with the increase of the content and molecular weight of PF, indicating that it was convenient to adjust the value of tan δ peak and the temperature range. FTIR studies provided positive evidence for the intermolecular hydrogen bonding between the PF hydroxyl groups and the ACM carbonyl groups, which made a great contribution to the damping properties. Compared with organic hybrids in our previous study, in which AO-80, a kind of organic small molecule was
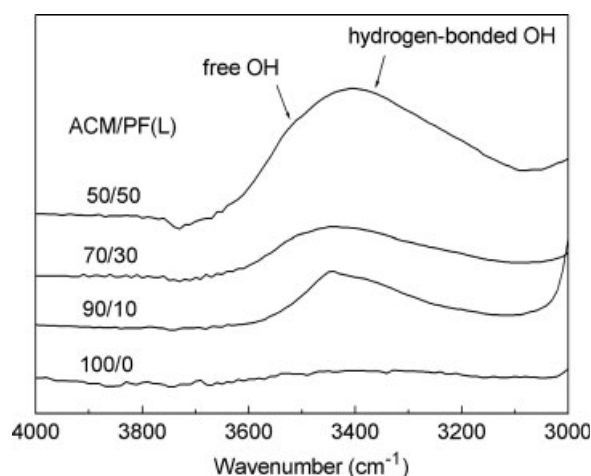
TABLE III
Damping Performance for Binary System of ACM/AO-80(50/50) and ACM/PF(50/50)

Blends (50/50)	tan δ peak value	tan δ peak temp. (°C)	Temp. range(°C) for tan δ > 1.00		
			T_1	T_2	ΔT
ACM/AO-80	4.00	25.0	14.0	50.0	36
ACM/PF(S)	2.05	43.0	27.0	67.0	40
ACM/PF(M)	1.95	49.0	34.0	73.0	41
ACM/PF(L)	1.74	54.0	37.0	81.0	44

Figure 9 FTIR spectra recorded at 4000–3000 cm^{-1} region at 25°C for ACM/PF(L).

applied, blends with PF got broader temperature ranges with higher flowing temperature, and should be more stable for practical application.

References

 1. Wu, C. F.; Yamajishi, T.; Nakamoto, Y.; Ishida, S. Polym Prep Jpn 1999, 48, 4169.
 2. Ratna, D.; Manoj, N. R.; Chandrasekhar, L.; Chakraborty, B. C. Polym Adv Technol 2004, 15, 583.
 3. Wang, X. D.; Zhang, Q. Chem J Chin Univ 2001, 22, 669.
 4. Shih, H. H.; Hamed, G. R. J Appl Polym Sci 1997, 63, 323.
 5. Dormidontova, E.; Brinke, G. Macromolecules 1998, 31, 2649.
 6. Byun, S. W.; Im, S. S. Polymer 1998, 39, 485.
 7. Fahrenholtz, S. R.; Kwei, T. K. Macromolecules 1981, 14, 1076.
 8. Grates, J. A.; Thomas, D. A.; Hickey, E. C.; Sperling, L. H. J Appl Polym Sci 1975, 19, 1731.
 9. Harris, J. A. Rubber Chem Technol 1989, 62, 515.
10. Sperling, L. H.; Fay, J. J Polym Adv Technol 1991, 2, 49.
11. Li, S. C.; Qiu, Q. W.; Jarvela, P. J Appl Polym Sci 2000, 76, 722.
12. Wei, Z.; Li, S. C. J Appl Polym Sci 2002, 84, 821.
13. Ogawa, T.; Koen, T.; Mukohyama, Y.; Inoue, S. J Soc Sci Jpn 1992, 41, 1569.
14. Wu, C. F. J Polym Sci Part B: Polym Phys 2001, 39, 23.
15. Wu, C. F. J Appl Polym Sci 2001, 80, 2468.
16. Wu, C. F.; Yamajishi, T.; Nakamoto, Y.; Ishida, S.; Nitta, K. J Polym Sci Part B: Polym Phys 2000, 38, 2943.
17. Wu, C. F.; Akiyama, S. Polym J 2001, 33, 955.
18. Wu, C. F.; Otani, Y.; Namiki, N.; Emi, H.; Nitta, K. Polym J 2001, 33, 322.
19. Wu, C. F. Chin J Polym Sci 2003, 21, 483.
20. Brown, K.; Hooker, J. C.; Creton, C. Macromol Mater Eng 2002, 287, 163.
21. Yamada, N.; Shoji, S.; Sasaki, A.; Nagatana, A.; Yamaguchi, K.; Kohjiya, S.; Hashim, A. S. J Appl Polym Sci 1999, 71, 855.
22. Yamada, N.; Shoji, S. J Polym Sci Part B: Polym Phys 2000, 38, 2285.
23. Huu, R.; Dimonie, V. L.; El-aasser, M. S.; Pearson, R. A.; Hiltner, A.; Mylonakis, S. G.; Sperling, L. H.; Fay, J. J Polym Sci Part B: Polym Phys 1997, 35, 1501.
24. Wu, H. D.; Chu, P. P.; Ma, C. C. M.; Chang, F. C. Macromolecules 1999, 32, 3097.
25. Wang, F. Y.; Ma, C. C. M.; Hung, A. Y. C.; Chang, F. C. Macromol Chem Phys 2001, 202, 2328.
26. Kuo, S. W.; Chang, F. C. Macromol Chem Phys 2001, 202, 3112.
27. Kuo, S. W.; Lin, C. L.; Chang, F. C. Macromolecules 2002, 35, 278.